S.1 Multiphysics modeling to verified the analytical diffusion coefficient

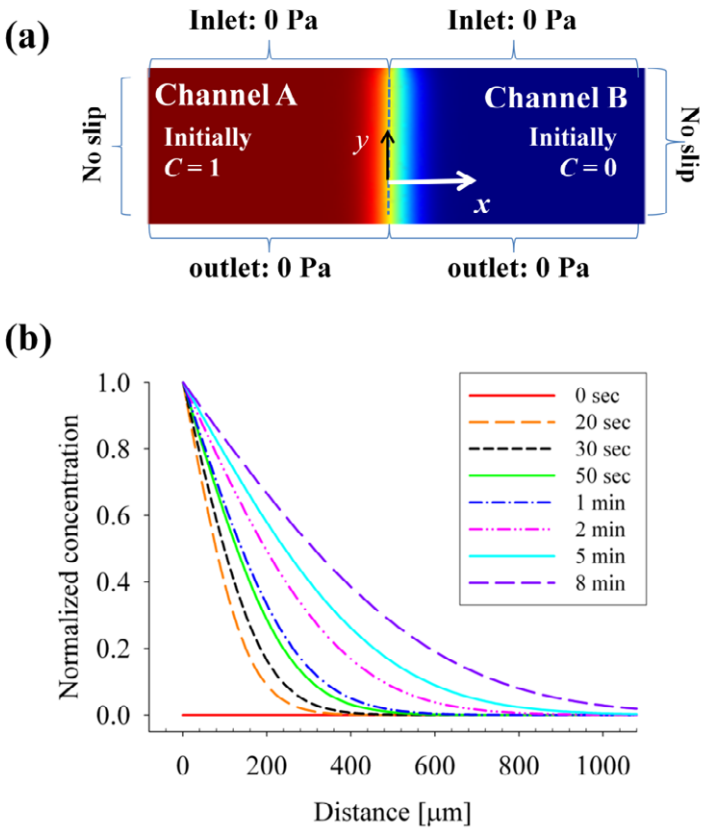

Fig. S1 (a) Schematic of the boundary condition for multiphysics simulation. **(b)** Multiphysics simulation results for this microchannel, taking into account the diffusion effect.

We verified this analytical diffusion coefficient using multiphysics modeling software (COMSOL Inc., Burlington, MA, USA). In this multiphysics modeling, we used the 4 mm by 1.5 mm computation channel shown in Fig. S1(a). We assumed that the normalized chemical concentrations in the two side channels, A and B, were initially fixed at C = 1 and 0, respectively, and that the entire system was governed by the time-dependent diffusion equation. The constant reference pressure of 0 Pa was used for the inlets and outlets: there was no mass flux at the inlets and outlets but only diffusion mixing occurred at the interfaces between the two chemicals. The mass flux is given by diffusion and convection, and the resulting mass balance equation is as follows:

$$\nabla \cdot \left(-D\nabla c + cu \right) = 0 \qquad \text{(S1)}$$

where D denotes the diffusion coefficient (m^2/s), c is the concentration (mol/m^3), and u is the velocity

vector (m/s). In here, the velocity is zero, hence the convective flux is zero. We used $D = 0.38 \times 10^{-9}$ m^2/s, which was derived using diffusion equation based on the experimental results. Fig. S1(b) describes the multiphysics simulation results for this microchannel. The simulation results showed good agreement with the experimental results, within 1 min. This result can be applied to quantitatively estimate the thicknesses of hydrogel membranes using the crosslinking reaction time-dependent method.

S.2 Single hydrogel membrane formation

S.2.1 Channel design and experimental setup

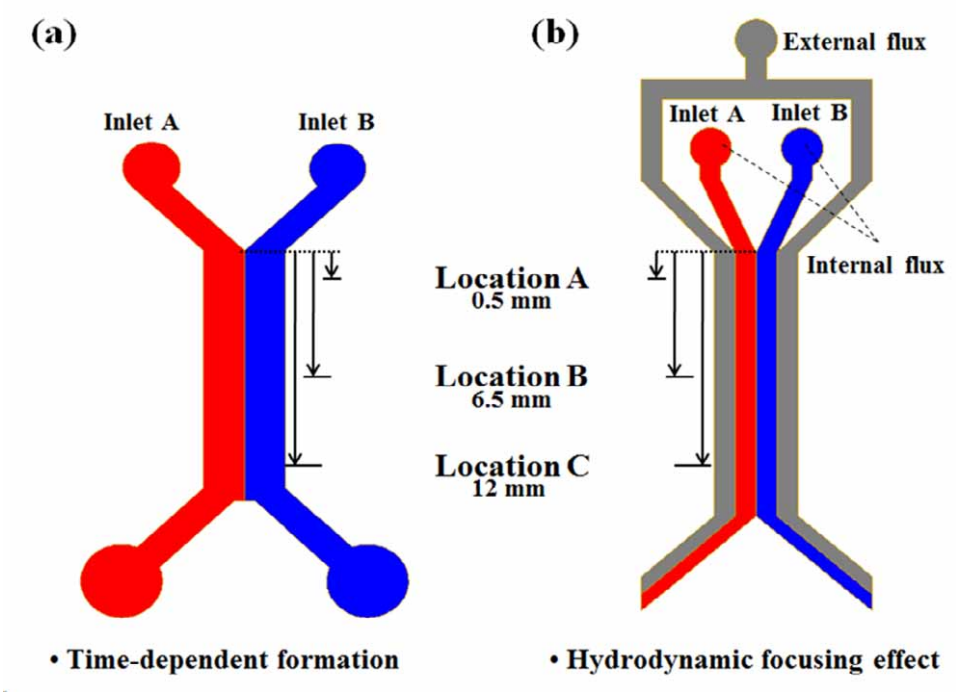

Fig. S2 Channels for controlling the thickness of the formed hydrogel membrane by **(a)** time-dependent methods, and **(b)** hydrodynamic focusing of the microfluidics.

Time-dependent formation of hydrogel membrane

We formed a single hydrogel membrane as a function of the crosslinking reaction time within the X-shaped microchannel: the width and length of the main channel were 4 and 13 mm, respectively (Fig. S2(a)). Two separate solutions: (1) 0.0625 wt% of H_2O_2 in PBS with Tet-SA-TA (5.2%) and (2) 0.0625 mg/mL of HRP in PBS with the same concentration of Tet-SA-TA (5.2%) were introduced at each inlet, respectively and filled the channel with the same flow rates (1.5 mL/min). Then, we waited a specific time (20, 30, or 50 s) and washed out the remainder of the two unreacted solutions using deionized water (DI water) at a flow rate of 0.5 mL/min.

Hydrodynamic focusing effect method

In addition to the gelation-time-dependent method, we also demonstrated the possibility of controlling the thickness of the *in situ* hydrogel membranes quantitatively by tuning the velocity of the microfluidics. Fig. S2(b) shows the scheme of a microfluidic chip designed for hydrodynamic focusing. The width and length of the channel were 4 mm and 13 mm, respectively. The external liquid streams were DI water, while the internal streams were the same two prepared solutions as above. These streams were maintained 60 s after fully filled the microchannel. The thickness of the

membranes could be controlled by varying the external/internal flow ratio. The internal volume flow rate was fixed at 1 mL/min, while the external/internal flow rate ratio was set at 1.0, 1.5, 2.0, and 2.5.

S.2.2 Time-dependent formation of hydrogel membrane

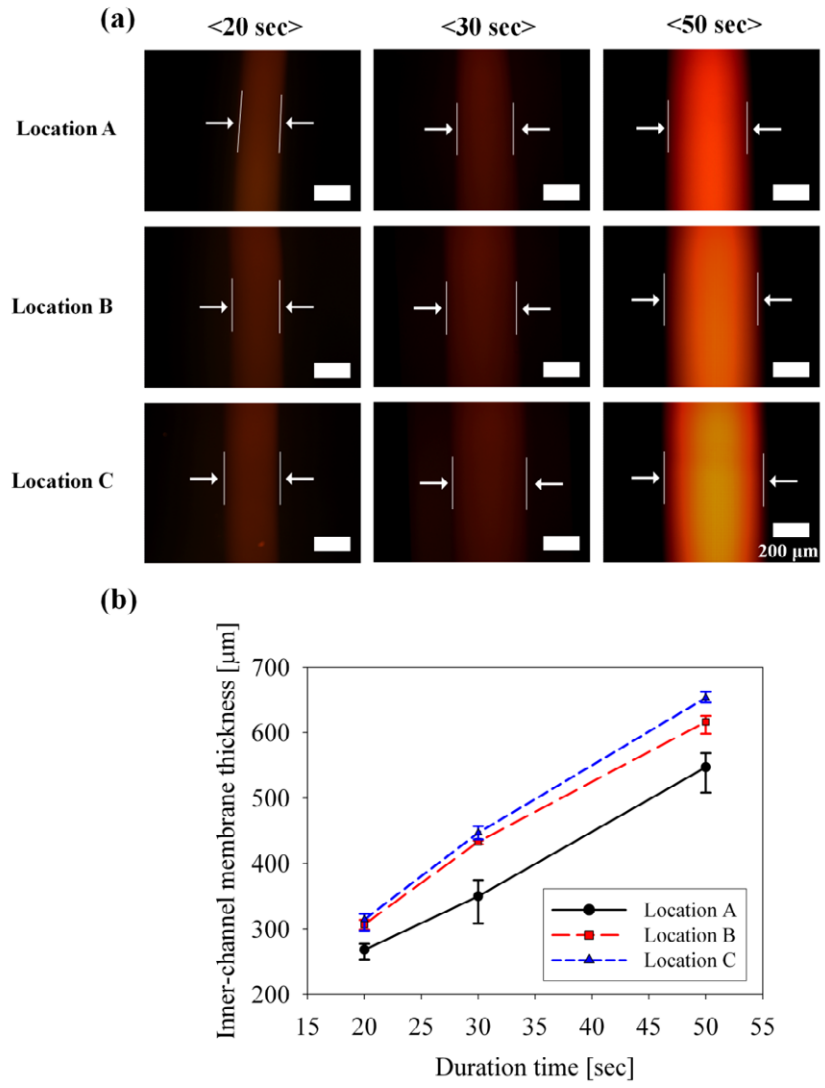

Fig. S3 (a) Pictures showing variation in membrane thickness of hydrogel membrane with respect to duration time (crosslinking reaction time). We repeated the experiments three times and measured the thicknesses of the hydrogel membrane at locations A, B, and C (locations A, B, and C are depicted in Fig. S2). **(b)** The corresponding plots for the relation between the gelation time and thickness of the membrane in the microchannel. All of the error bars represent the standard deviation.

Fig. S3(a) shows images of the hydrogel membranes formed in microchannels with variations in crosslinking reaction time, while Fig. S3(b) shows the corresponding plots representing the variations

in thickness according to the crosslinking reaction time. (a) At 20 s after the reaction, the thicknesses of the membrane at locations A, B, and C were 268 ± 9, 307 ± 7, and 314 ± 9 μm, respectively. (b) At 30 s after the reaction, the thicknesses of the membrane at locations A, B, and C were 350 ± 24 μm, 433 ± 2 μm, and 447 ± 10 μm, respectively. (c) At 50 s after the reaction, the thicknesses of the membrane at locations A, B, and C were 547 ± 22 μm, 617 ± 9 μm, and 653 ± 9 μm, respectively. Because the channel was filled using two laminar solution flows from the inlets, it is obvious that more molecules were diffused as the measurement location moved toward the end of the microchannel; that is, the thickness of the hydrogel membrane increased around the end of the microchannel. The thickness can be roughly estimated using the following analytical approaches.

Basically, the thickness of the membrane at the interface between two separated solutions by crosslinking reaction time, W_c, is reconstructed from equation (1):

$$W_c = 2\sqrt{2tD} \tag{S2}$$

where t is the crosslinking reaction time. However, since the time for fully filled the length of the channel provides additional crosslinking reaction time, thickness of the membrane during filled the channel, W_f, can be derived as follows.

The volume flow rate in the microchannel can be given by

$$Q = AV \tag{S3}$$

here, Q is the volume flow rate, A is the cross-sectional area of the microchannel, and V is the velocity of the flow. V can be reconstructed as l/τ, where l is the length from the inlet to the measurement location and τ is the average diffusion time[1]. Then, by substituting equation (S3) into equation (1), the additional thickness of the membrane during filled the channel, W_f, can be derived using the following equation:

$$W_f = 2\sqrt{\frac{2AlD}{Q}} \tag{S4}$$

Because the crosslinking reaction occurs in both directions from the interface of the two solutions, the thickness of the membrane should be twice the relevant mixing path.

As a consequence, the total thickness of the formed hydrogel membrane, W, at l is derived as the sum of equations (S2) and (S4):

$$W = W_c + W_f = 2(\sqrt{2tD} + \sqrt{\frac{2AlD}{Q}}) \quad \text{(S5)}$$

Because A is 4 mm × 50 μm, the diffusion coefficient D is 0.38 × 10^{-9} m^2/s, and Q is 0.5 mL/min, the thicknesses are calculated as follows. (a) At 20 s after the reaction, the thicknesses of the membrane at locations A, B, and C are 255 μm, 269 μm, and 276 μm, respectively. (b) At 30 s after the reaction, the thicknesses of the membrane at locations A, B, and C are 311 μm, 325 μm, and 332 μm, respectively. (c) At 50 s after the reaction, the thicknesses of the membrane at locations A, B, and C are 398 μm, 412 μm, and 419 μm, respectively. A comparison of the analytical and experimental results for the thicknesses shows differences of 6–55%. However, because there was a time delay (<10 s) to change the syringe with DI water for washing out the unreacted solutions, we had already expected this discordance. This time delay may increase the thickness of the membrane by approximately 54%. The calculations therefore show good agreement with the experimental results. In any case, to reduce the disagreement and obtain an accurate estimation, it is necessary to use an experimental setup that allows a rapid and stable shift from the two solution flows to DI water, e.g., a three-way valve system.

S.2.3 Hydrodynamic focusing effect method

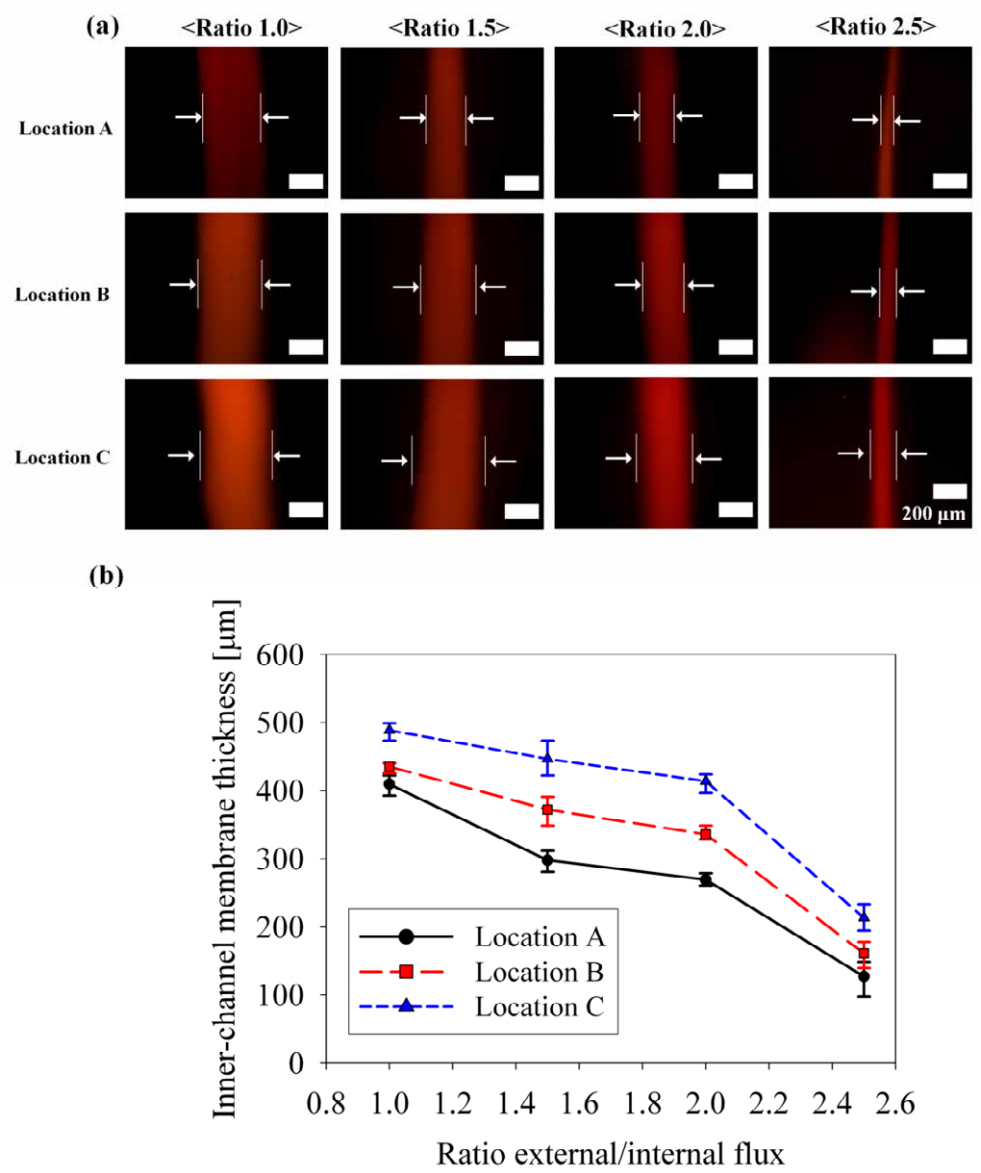

Fig. S4 (a) Optical images of membrane quantitatively controlled by adjusting velocities of microfluidics. **(b)** The membrane thickness is a function of the external/internal stream ratio. We repeated the experiments three times and measured the thicknesses of the hydrogel membrane at locations A, B, and C. All of the error bars represent the standard deviation.

In order to control the thickness of the hydrogel membrane, the hydrodynamic focusing effect was also applied by tuning the flow rate ratio (external/internal). Fig. S4(a) shows optical images of membranes controlled using the proposed method. We repeated the experiments three times and measured the thicknesses of the hydrogel membranes at locations A, B, and C. (a) At a flow rate ratio

of 1.0, the thicknesses of the membrane at locations A, B, and C were 407 ± 14 μm, 433 ± 7 μm, and 486 ± 12 μm, respectively. (b) At a ratio of 1.5, the thicknesses of the membrane at locations A, B, and C were 296 ± 15 μm, 369 ± 21 μm, and 447 ± 25 μm, respectively. (c) At a ratio of 2.0, the thicknesses of the membrane at locations A, B, and C were 269 ± 9 μm, 338 ± 10 μm, and 410 ± 13 μm, respectively. (d) At a ratio of 2.5, the thicknesses of the membrane at locations A, B, and C were 122 ± 25 μm, 158 ± 19 μm, and 213 ± 19 μm, respectively. We plotted this variation in the membrane thickness as a function of the external/internal stream ratio, as shown in Fig. S4(b). A wider membrane was observed as the measurement location moved toward the end of the microchannel, while the membrane was inclined to become narrower when the external/internal stream ratio increased.

S.3 Multiphysics simulation for permeability study

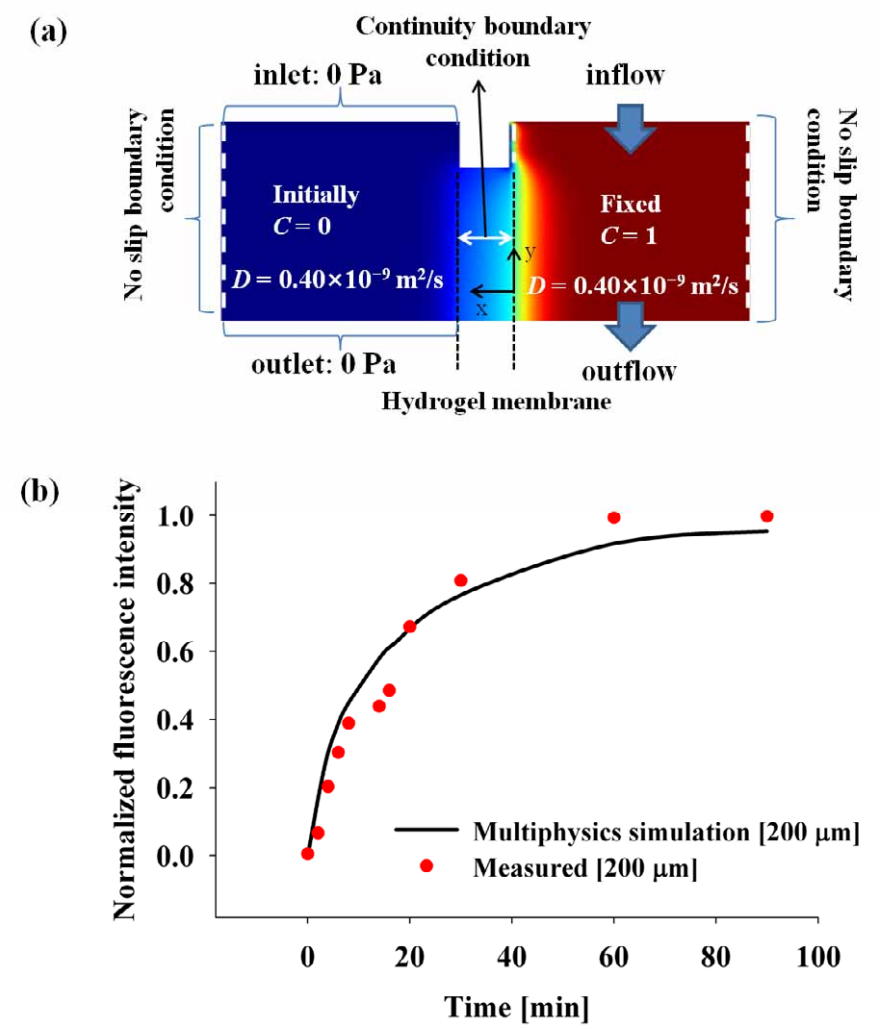

Fig. S5 (a) Concentration field within left channel computed using multiphysics modeling. These results revealed the value of the diffusion coefficient of the chemical (Dylight 549) in the hydrogel membrane. **(b)** Multiphysics simulation results compared with experimental results.

The concentration field within the left channel was computed using the multiphysics simulation, and the diffusion coefficient of the chemical (Dylight 549) in the hydrogel membrane was verified. In this multiphysics modeling, we used a computation channel with the same dimensions as real microfluidic channels. The width of the left and right channels was 1.82 mm, and the hydrogel membrane thickness was 360 μm in the middle of the channel. We assumed that the normalized chemical concentrations at the left and right channels were fixed at C = 0 and 1, respectively. A constant reference pressure of 0 Pa was set at the inlet and outlet of the left side of the channel; that is, there was no net flow of DI water.

In addition, because the diffusion coefficient for the Dylight 549 in the DI water at the left channel was needed for the simulation, we needed to estimate its value in the following experiment using the X-shaped channel in Fig. S2(a). DI water and the fluorescence dye were injected into each inlet with two laminar solution flows at the same volume flow rate, 1.0 mL/min. Because more molecules were diffused as the flow moved toward the end of the microchannel, we could measure the different relevant mixing paths based on the position in the microchannel. Then, we calculated the diffusion coefficient of the fluorescence dye in DI water using equation (S5) and found its value to be approximately 0.40×10^{-9} m^2/s. These results are similar to the diffusion coefficients reported for analogous fluorescence dyes such as Atto655, Atto488, Rhodamine 6G, Rhodamine B, Fluorescein, and Oregon green 488 in water: their average value is 0.40×10^{-9} m^2/s[2-4].

At the right side channel, in order to maintain the concentration, $C = 1$, an inflow rate of 1.0 μL/min was used at the inlet, and the other boundary conditions are as depicted in Fig. S5(a). Fig. S5(b) shows the multiphysics simulation results compared with the experimental results in the left side channel at 200 μm from the left edge of the membrane ($x = 0$). The dots represent the measured values and the solid line is based on the multiphysics simulation. The simulation results showed good agreement, where the diffusion coefficient of the fluorescence dye in the hydrogel membrane was 1.62×10^{-9} m^2/s.

S.4 Multiphysics simulation to verify the discrepancy between the theoretical and experimental results

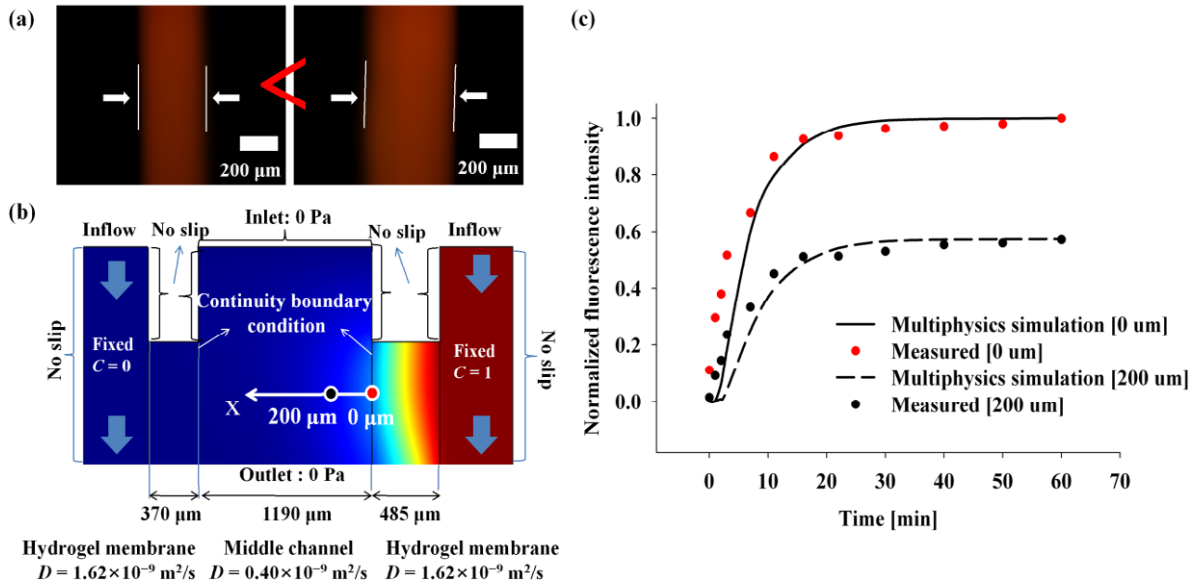

Fig. S6 (a) Optical pictures of formed parallel membranes in the same region. The thickness of the membrane on the right side is 31% larger than that on the left side. **(b)** Schematic of the boundary condition for multiphysics simulation. **(c)** Multiphysics simulation results compared with experimental results

In this multiphysics modeling, we used the computation model shown in Fig. S6(b), which is based on the actual sizes of channels and membranes. We assumed that the normalized chemical concentration, C, within the two sides of channels A and B were initially fixed at $C = 0$ and 1, respectively, and in order to maintain these concentrations, an inflow rate of 1.0 μL/min was set at each inlet. The center of the channel was fixed at $C = 0$ and a constant reference pressure of 0 Pa was used at the inlet and outlet to stop the flow. In addition, the other boundary conditions were as depicted in Fig. S6(b), and the entire system was governed by the time-dependent diffusion equation. Fig. S6(c) shows a comparison of the simulation and experimental data in the center of the channel at 0 and 200 μm from the left edge of the membrane on the right side ($x = 0$). The dots represent the measured values and the two lines depict the simulation results. The simulation results showed good agreement with the experimental results.

Reference

1. N.-T. Nguyen and S. T. Wereley, *Fundamentals and Applications of Microfluidics*, Artech House Inc., Boston/London, 2002.
2. C. B. Muller, A. Loman, V. Pacheco, F. Koberling, D. Willbold, W. Richtering and J. Enderlein, *Epl*, 2008, **83**, -.
3. C. T. Culbertson, S. C. Jacobson and J. M. Ramsey, *Talanta*, 2002, **56**, 365-373.
4. P. O. Gendron, F. Avaltroni and K. J. Wilkinson, *Journal of Fluorescence*, 2008, **18**, 1093-1101.